Thermodynamic Analysis and Performance Evaluation of a Proposed Novel Combined Cooling and Power System

John Carlo S. Garcia, Menandro S. Berana
Department of Mechanical Engineering, College of Engineering,
University of the Philippines, Diliman, Quezon City, 1101, Philippines

Abstract — *A novel combined cooling and power (CCP) system, wherein an organic Rankine cycle is coupled with a compressor-driven ejector refrigeration cycle, is proposed. The ejector primary flow of this refrigeration system comes from one of the streams that is pumped from the condenser, which is unconventional from the existing studies wherein the turbine exhaust is its primary flow source. Parametric analysis was conducted to study the effects of the heat source and evaporator temperature, and entrainment ratio on the coefficient of performance (COP) and exergy efficiency of the proposed system using three working fluids, namely R123, R141b, and R245fa. In the novel setup, the COP improvement can be theoretically associated to the produced turbine power that reduces the power input to the system. Among the parameters observed, the entrainment ratio and evaporator temperature had the greatest effect on the performance of the system. The system exergy efficiency varies inversely with entrainment ratio and evaporator temperature; on the other hand, the COP improves with the increase in the evaporator temperature and decrease in the entrainment ratio. The performance of three working fluids was also investigated. Among the three refrigerants, the system that used R141b had the highest COP and exergy efficiency at 3.26 and 46.92%, respectively.*

Keywords — combined cooling and power system, ejector, exergy analysis

I. INTRODUCTION

Research on low-grade heat utilization has drawn much attention and become increasingly popular in recent years. It has shown several effects on the improvement of overall energy conversion efficiency and reduction of global environmental-related problems such as greenhouse gas emission.

Low-grade heat, as defined by the U.S. Department of Energy [1], has temperature below 232 ^{o}C. Its primary sources are biomass, geothermal, solar, and waste heat energy. Waste heat from industrial plants is a byproduct of combustion and chemical processes, and is directly exhausted to the environment. According to the Philippine Power Statistics published by the Department of Energy, approximately one-third of the energy consumption comes from the industrial sector [2]. Among the Philippine industrial sectors, food processing and manufacturing (36.2%), cement and constructions (27.4%), and mining, minerals and metals processing (12.2%) have the high energy demands [3]. Stricker et al. conducted a study on the eight largest manufacturing sectors in Canada, and concluded that approximately 70% of the input energy is released to the environment [4]. Based on these reports, it is clearly seen that the industrial sector has high energy consumption and wastage.

Studies on waste heat recovery systems are usually employed in the industrial sector, and the key parameters observed in waste heat streams are their matter state and composition, temperature, mass flowrate, and availability [5]. Some of the identified waste streams are flue or exhaust gas from furnaces, gas engines and thermal post combustion, pressurized hot water, and exhaust vapors [6]. These waste streams are used in recovery systems that have various applications such as power generation, refrigeration, and desalination.

Several recent research studies have focused on the power generation from low-grade heat recovery systems. Most of them concentrated on organic Rankine cycle (ORC) [7-9], supercritical or transcritical cycles [10-12], and thermodynamic cycles using unconventional working fluids [13-15]. Meanwhile, the absorption cycle has the greatest number of recent studies among the refrigeration systems [16-18]. Aside from power generation and refrigeration, waste heat recovery systems have also been explored for cogeneration such as combined heating and power (CHP), combined cooling, heating, and power (CCHP), and combined cooling and power (CCP) applications.

The focus of this study is on the low-grade heat utilization in a CCP system. The commonly used power cycles in a CCP system in literatures are the Rankine cycle, the organic Rankine cycle, and the Kalina cycle; on the other hand, the vapor compression cycle, absorption cycle, and the ejector cycle are the often-used refrigeration cycles. There are many possible configurations of power-and-refrigeration systems, but this study specifically investigates the performance of an organic Rankine-ejector refrigeration CCP system.

Alexis studied a cogeneration system where the bled turbine steam of a Rankine cycle is supplied to a heat generator of the ejector refrigeration system [19]. Dai et al., and Zheng and Weng investigated the same system that couples the Rankine cycle with the ejector refrigeration cycle, and used R123 and R245fa, respectively, as working fluids [20,21]. In their configuration, a turbine is added in between the heat recovery vapor generator and ejector. Both studies evaluated the performance of the CCP system using exergy efficiency, and concluded that there is a great amount of exergy loss in the ejector. Yang et al. adopted the system of Dai, but a zeotropic mixture of isobutane-pentane was used as the working fluid [22]. Wang et al. also proposed a similar system to Dai et al., and Zheng and Weng except that it requires a preheater [23]. A comparative study of the performance of different working fluids was conducted by Habibzadeh et al. employing the system proposed by Wang. Their research showed that R601 has the highest thermal efficiency (14.24%) among the five working fluids observed [24]. Most of the researches on CCP systems with ejector refrigeration cycle are of heat-driven type. The primary flow of the ejector comes from either the turbine outlet or bled steam, and the evaporator exit stream as the secondary flow.

In this study, the proposed power-and-refrigeration system uses compressor-driven ejector refrigeration cycle. One of the streams that are pumped from the condenser outlet acts as the ejector primary flow, while the combined streams of turbine and evaporator outlet as the secondary flow. The turbine power is maximized in the proposed system compared to the heat-driven type because of the pressure difference observed in the cycle.

The performance of the proposed system using R123, R141b, and R245fa is evaluated. These three working fluids are chosen for their good thermodynamic and physical properties, and also for their low ozone depletion potential (ODP), global warming potential (GWP), and atmospheric lifetime (ALT). Parametric analysis is also conducted to investigate the effects of the heat source and evaporator temperature, and the entrainment ratio on the coefficient of performance (COP) and exergy efficiency of the system.

II. SYSTEM DESCRIPTION AND ASSUMPTIONS

The proposed combined cooling and power system couples organic Rankine cycle with compressor-driven ejector refrigeration cycle. The system consists of nine components: compressor, condenser, pump, vapor generator, turbine, ejector, vapor-liquid separator, throttle valve and evaporator. Figures 1 and 2 illustrate the schematic and temperature-specific entropy (*T*-*s*) diagrams of the system.

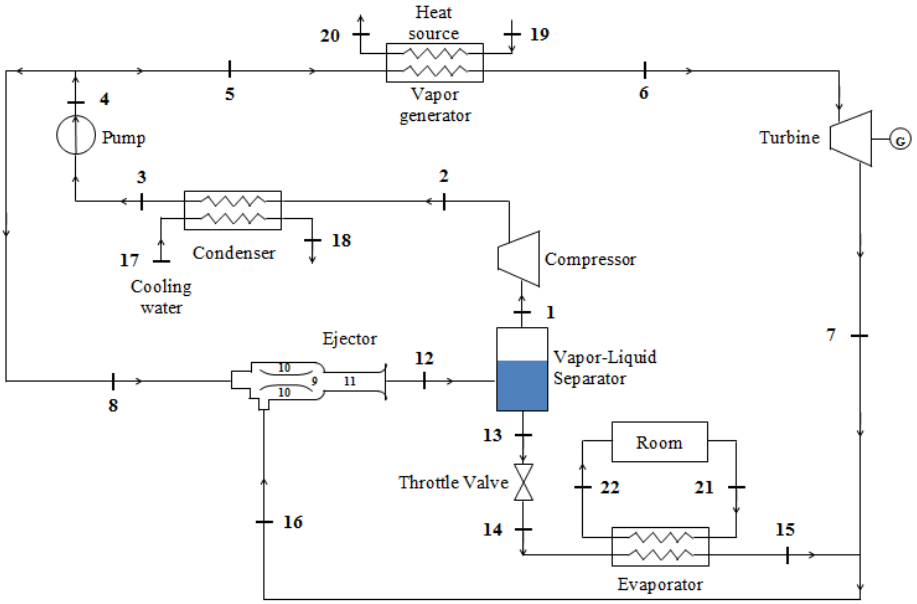

Figure 1. Schematic diagram of the proposed combined power-and-refrigeration system

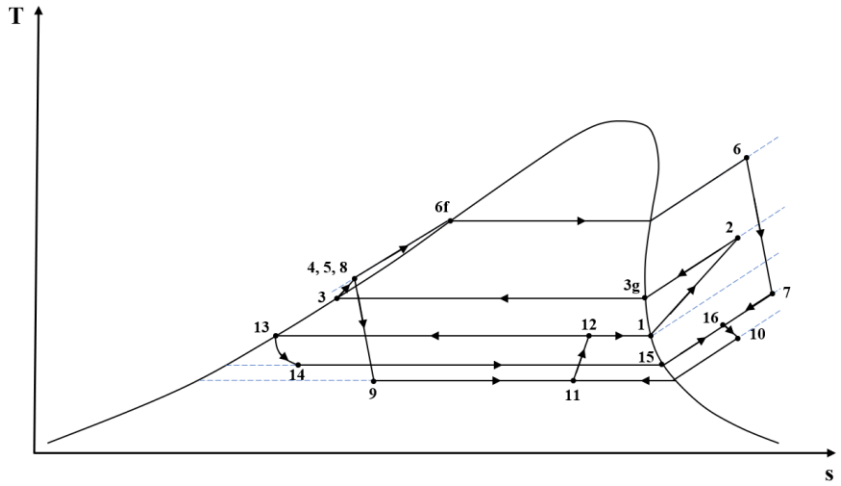

Figure 2. T-s diagram of the proposed combined power-and-refrigeration cycle

Saturated vapor working fluid (state 1) flows through the compressor, which raises its pressure to the condenser pressure level (state 2). The superheated working fluid is then cooled at the condenser (state 3) by giving off heat to the cooling water. After that, the working fluid is pumped to a high pressure (state 4), and is divided into two streams— one stream serves as the primary flow of the ejector (state 8), and the other stream (state 5) goes to the power side of the system. The high-pressure compressed liquid (state 5) is vaporized at the vapor generator by absorbing heat from a waste heat stream, which is assumed to be air. The high-pressure, high-temperature vapor (state 6) is expanded in the turbine consequently producing mechanical power. The saturated liquid working fluid (state 13) from the vapor-liquid separator is throttled to the evaporator pressure level (state 14). This saturated mixture then passes through the evaporator and vaporizes as it absorbs heat from the air that comes from the refrigerated space. The stream of saturated vapor that exits the evaporator (state 15) is mixed with the fully expanded stream of vapor from the turbine (state 7), and the resulting stream of low-pressure superheated vapor (state 16) becomes the secondary flow of the ejector. The high-pressure stream (state 8) that enters the ejector accelerates to supersonic conditions (state 9) as it passes through the converging-diverging nozzle. This creates a low-pressure region at the nozzle exit which in effect entrains the low-pressure stream (state 10). The streams of primary and secondary flows mix in the constant-area chamber (state 11), and recovers pressure at the diffuser (state 12). The stream of working fluid that exits the ejector is then separated to saturated vapor (state 1) and saturated liquid (state 13) in the vapor-liquid separator.

The following assumptions are made for the system simulation:

(1) The system is at steady state.
(2) The difference in the kinetic and potential energies as well as pressure drops in pipes are neglected. Heat losses at the condenser, compressor, ejector, evaporator, turbine, and vapor generator are also considered negligible.
(3) The throttling process is isenthalpic.
(4) The streams of working fluids that exit the condenser and evaporator are saturated liquid and saturated vapor, respectively.
(5) The exit states at the vapor-liquid separator are saturated.

(6) The temperature difference between the working fluid and the external fluid at the inlet of each heat exchanger (condenser, evaporator, and vapor generator) is set to 10 ^{o}C, while pinch-point temperature difference in the heat exchangers is equal to 5 ^{o}C.

The assumed values of each operating parameters are summarized in Table 1.

Table 1. Conditions assigned to system parameters

Environment temperature	T_o = 27 ^{o}C
Environment pressure	P_o = 101.325 kPa
Turbine inlet pressure	P_6 = 650 kPa
Turbine isentropic efficiency	η_t = 0.80
Compressor isentropic efficiency	η_c = 0.80
Pump isentropic efficiency	η_p = 0.80
Heat source inlet temperature	T_{19} = 120 ^{o}C
Cooling water inlet temperature	T_{17} = 27 ^{o}C
Evaporation temperature	$T_{14} = T_{15}$ = -5 ^{o}C
Refrigerating capacity	$\dot{Q}_e$ = 100 kW

III. SYSTEM MODELING EQUATIONS

The key component in the proposed cycle is the ejector, and it is modeled using methods employed by Garcia et al. [25]. The ejector profile modeling has the following assumptions:

(1) The flow inside the ejector is in steady-state, and is modeled and simulated as one-dimensional.
(2) For the two-phase region, the flow is assumed to be homogenous.
(3) The mixing of the primary and secondary flows in the mixing chamber is isobaric.
(4) The ejector does not experience shock.

The law of conservation of energy, considering the previously stated assumptions, is observed in each component; thus, the following equations are obtained:

- For the vapor-liquid separator,

$$\dot{m}_{12}h_{12} = \dot{m}_1h_1 + \dot{m}_{13}h_{13} \tag{1}$$

- For the compressor,

$$\dot{W}_c = \dot{m}_1(h_2 - h_1) \tag{2a}$$

$$\eta_c = \frac{h_{2s} - h_1}{h_2 - h_1} \tag{2b}$$

- For the condenser,

$$\dot{Q}_k = \dot{m}_2(h_2 - h_3) = \dot{m}_{17} c_{p,w}(T_{18} - T_{17}) \quad (3)$$

- For the pump,

$$\dot{W}_p = \dot{m}_3(h_4 - h_3) \quad (4a)$$

$$\eta_p = \frac{h_{4s} - h_3}{h_4 - h_3} \quad (4b)$$

- For the vapor generator,

$$\dot{Q}_{vg} = \dot{m}_5(h_6 - h_5) = \dot{m}_{19} c_{p,a}(T_{19} - T_{20}) \quad (5)$$

- For the turbine,

$$\dot{W}_t = \dot{m}_6(h_6 - h_7) \quad (6a)$$

$$\eta_t = \frac{h_6 - h_7}{h_6 - h_{7s}} \quad (6b)$$

- For the evaporator,

$$\dot{Q}_e = \dot{m}_{14}(h_{15} - h_{14}) = \dot{m}_{21} c_{p,w}(T_{21} - T_{22}) \quad (7)$$

- For the mixing of streams 7 and 15,

$$\dot{m}_7 h_7 + \dot{m}_{15} h_{15} = \dot{m}_{16} h_{16} \quad (8)$$

The proposed combined cooling and power system mainly functions as a refrigeration system. The performance of the system can be therefore evaluated using coefficient of performance (COP), which is defined as the ratio of the refrigerating capacity to the input of the system. For the proposed system, the two inputs are the heat extracted at the vapor generator and the power requirement of the system. Thus, the COP is expressed as

$$COP = \frac{\dot{Q}_e}{\dot{W}_{net,ref} + \dot{Q}_{vg}} \quad (9)$$

where

$$\dot{W}_{net,ref} = \left|\left|\dot{W}_c + \dot{W}_p\right| - \dot{W}_t\right| \quad (10)$$

Most of the researchers that studied combined power and refrigeration systems agree that the exergy efficiency is a better system performance evaluator compared with the first law efficiency (thermal efficiency and COP). The latter treats both mechanical power and heat equal, while the former differentiates these two forms of energies in terms of irreversibility.

Exergy is defined as the maximum amount of useful work that can be obtained from a system at a given reference environment [26]. In this study, the specified dead states are the reference pressure P_0 and temperature T_0. The following assumptions are made in the exergy analysis:

(1) Only physical exergies are accounted for the waste heat source and stream flows.
(2) Chemical, kinetic, and potential exergies are neglected.

With the given assumptions, the exergy of each state point is calculated as

$$E_n = m_n[(h_n - h_o) - T_o(s_n - s_o)] \tag{11}$$

The exergy efficiency is the ratio of the exergy output to the exergy input. The net work requirement and the available heat exergy exchange of the waste heat source are the exergy inputs of the system while the exergy output is the exergy of refrigeration. Exergy efficiency is therefore given as

$$\eta_{exg} = \frac{E_e}{W_{net,ref} + E_{hs}} \tag{12}$$

The exergy balance in each component can be expressed as

$$I = \sum E_{in} - \sum E_{out} \tag{13}$$

where *I* is the exergy destruction, or also known as irreversibility. The exergy destruction for each component is estimated by

- For the ejector,
$$I_j = E_8 + E_{16} - E_{12} \tag{14}$$
- For the vapor-liquid separator,
$$I_{sep} = E_{12} - E_1 - E_{13} \tag{15}$$
- For the compressor,
$$I_c = E_1 + \dot{W}_c - E_2 \tag{16}$$
- For the condenser,
$$I_k = E_2 + E_{17} - E_3 - E_{18} \tag{17}$$
- For the pump,
$$I_p = E_3 + \dot{W}_p - E_4 \tag{18}$$
- For the vapor generator,
$$I_{vg} = E_{in,vg} + E_5 - E_{out,vg} - E_6 \tag{19}$$
- For the turbine,
$$I_t = E_6 - \dot{W}_t - E_7 \tag{20}$$
- For the throttle device,
$$I_{td} = E_{13} - E_{14} \tag{21}$$

It is also important to observe the splitting of stream 4 into streams 5 and 8, and also the mixing of streams 7 and 15 into stream 16. Since streams 4, 5, and 8 have identical properties, there is no exergy destruction. However, for the case of the mixing of the two streams, its exergy destruction is expressed as:

$$I_{mix} = E_9 + E_{17} - E_{18} \tag{22}$$

IV. SOLUTION PROCEDURE

The steps for the mathematical solution of the system are as follows:

1. Input the working parameters: T_o, P_o, P_6, η_t, η_c, η_p, T_{15}, T_{17}, T_{19}, ΔT, and $\dot{Q}_e$.
2. Choose desired entrainment ratio (ω) and quality of the ejector outlet, x_{12}.
3. Obtain the mass flowrate and thermodynamic properties of the working fluid in each state point of the cycle.
4. Separator temperature is initially set at the evaporating temperature. From the given separator temperature, it will output a value of x'_{12}.
5. The separator will increase by 0.01°C until it satisfies the condition
$$\left|x_{12,desired} - x'_{12}\right| < 0.0001.$$
6. Check whether the entropy generated at the ejector is positive. If not, vary the value of the desired x_{12}.
7. Obtain the mass flowrate and thermodynamic properties of the external fluids in each state point.
8. Calculate the values of $\dot{W}_t$, $\dot{W}_c$, $\dot{W}_p$, and the exergy destruction of each device.
9. Calculate the COP and exergy efficiency of the cycle.

The solution procedure for evaluating the system performance is also summarized in Figure 3.

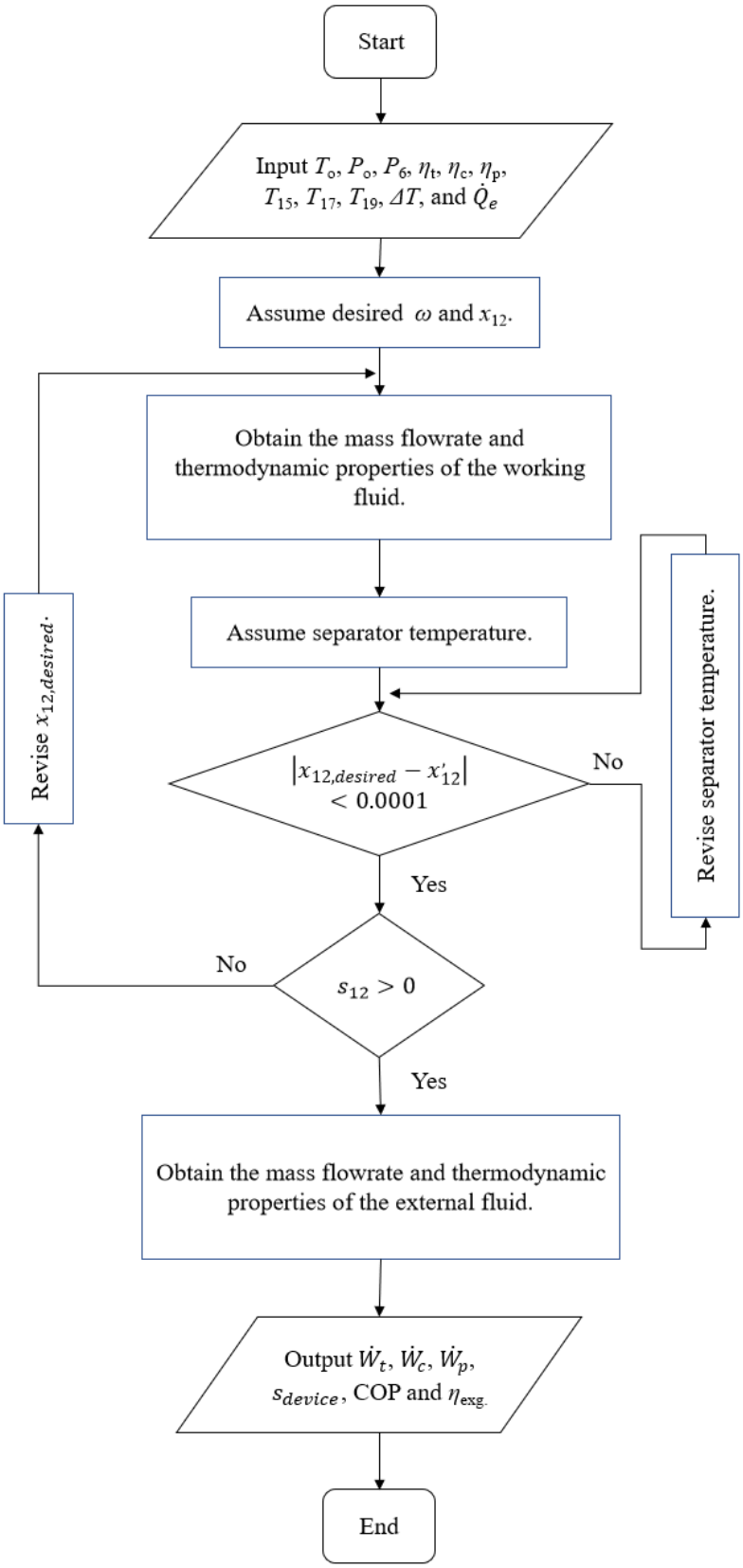

Figure 3. Simulation flowchart of system performance evaluation

V. RESULTS AND DISCUSSION

For the two-phase flow computation used in this study, the computational technique, which uses established equation of state [27] and Blasius friction factor [28] as incorporation in the conservation equations, has been found to give good agreement with the computational results of Berana and Bermido [29], Espeña and Berana [30], and Redo et al. [31], and the experimental results of Berana [32,33] in the nozzle decompression. The mentioned satisfactory prediction gave confidence on the high probability of the behavior of the two-phase flow obtained in the study. The simulation of the proposed CCP system was carried out using developed codes run through Python [34], and thermodynamic properties were obtained using CoolProp [27].

The system is first simulated using the assumed values of operating parameters in Table 1, and an entrainment ratio of 0.90. The performance of the system using R123, R141b, and R245fa for the base case scenario is summarized in Table 2. It is observed that the fluid with a higher critical temperature yields higher coefficient of performance. Among the three working fluids, R141b is considered the best for it has the highest COP and requires the lowest mass flowrate.

It is also seen in Table 2 that the compressor has the highest exergy destruction among the nine components. This is attributed to the large power requirement caused by the incapability of the ejector to raise the back pressure. Hence, the working fluid enters the condenser at an elevated temperature. The large temperature difference between the working fluid and cooling water may have resulted in the high exergy destruction in the condenser.

Table 2. Performance of the proposed system using the three working fluids

Parameter	R123	R141b	R245fa
$\dot{m}_{total}$ (kg/s)	1.35	0.99	1.28
I_c (kW)	4.28	4.00	4.67
I_j (kW)	0.01	0.01	0.00
I_k (kW)	3.29	3.23	3.52
I_p (kW)	0.07	0.06	0.06
I_{sep} (kW)	0.02	0.02	0.01
I_t (kW)	0.91	0.67	1.15
I_{td} (kW)	0.03	0.02	0.04
I_{vg} (kW)	0.99	0.73	1.60
$\dot{W}_c$ (kW)	22.36	21.36	24.22
$\dot{W}_p$ (kW)	0.35	0.31	0.32
$\dot{W}_t$ (kW)	3.66	2.54	4.94
$\dot{Q}_{vg}$ (kW)	17.42	19.13	27.26
COP	2.74	3.26	2.13
η_{exg} (%)	46.06	46.92	45.73

In order to investigate the effects of the entrainment ratio, and heat source and evaporating temperatures on the performance of the system, parametric analysis was conducted, which is discussed in the next subsections.

5.1. Effects of Entrainment Ratio

The entrainment ratio was varied from 0.85 to 0.975 with an increment of 0.125, while other parameters were held constant. The change in the compressor and turbine power, and the change in the heat exchange at the vapor generator with respect to the entrainment ratio are illustrated in Figure 4. It is observed that the ejector back pressure decreases with the increase of entrainment ratio, which may result in the increase of the total mass flowrate of the system. With the lower ejector outlet pressure, the compressor requires more power. Moreover, there is also an increase in the fraction of the mass flowrate that goes to the vapor generator and turbine. Thus, higher entrainment ratio indicates larger turbine power and vapor generator heat duty.

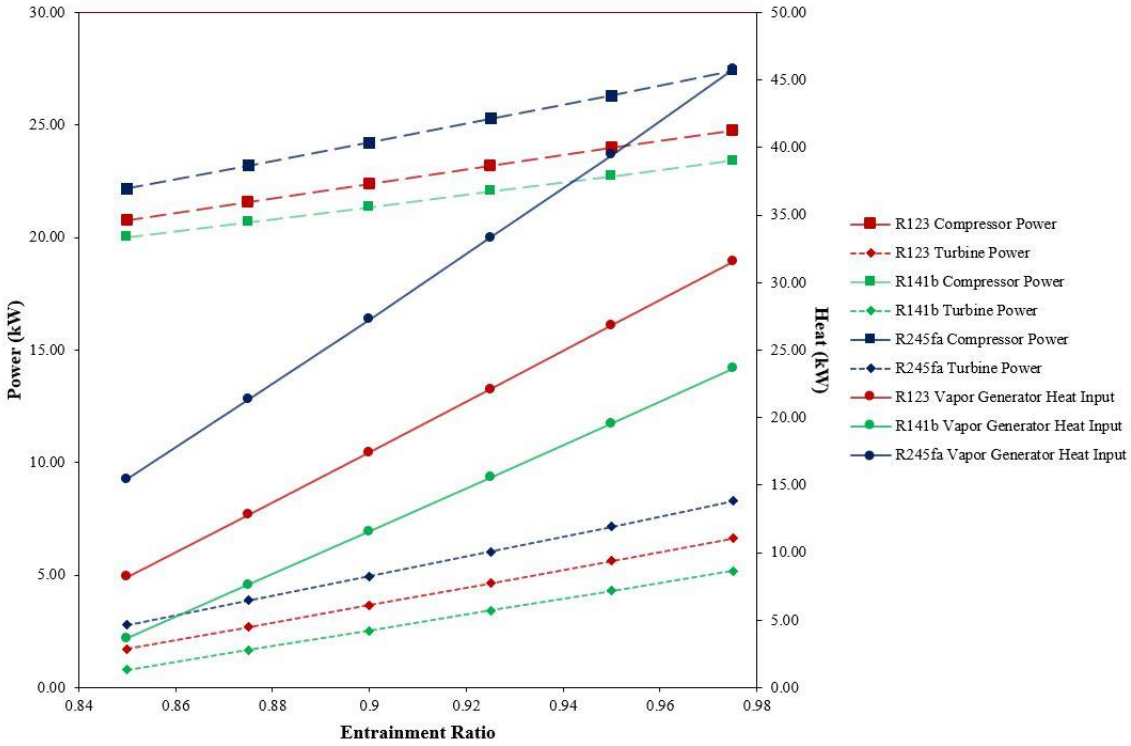

Figure 4. Effect of entrainment ratio on compressor and turbine power, and to the heat duty of the vapor generator

The performance of the proposed system with varying entrainment ratio is shown in Figure 5. The increase in entrainment ratio may result in lower coefficient of performance. Even though there is lower required net cycle power, the heat duty of the vapor generator is higher. Moreover, the exergy input of the system is increased with higher heat source flowrate. Accordingly, the exergy efficiency decreases with the increase in entrainment ratio.

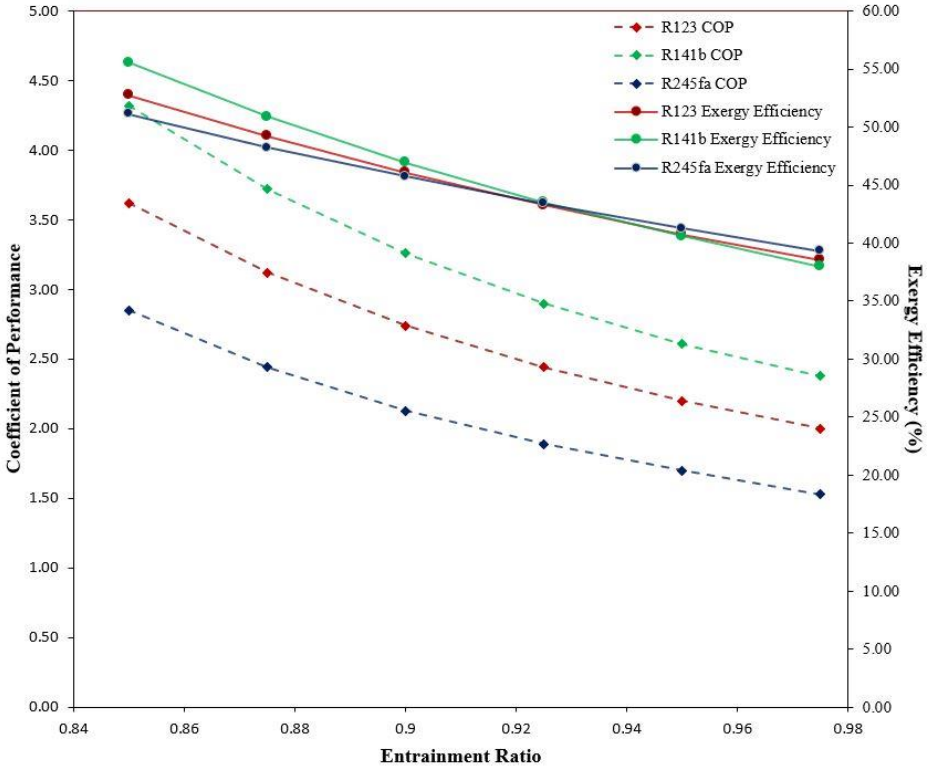

Figure 5. Effect of entrainment ratio on the COP and η_{exg} of the system

5.2. Effects of Heat Source Temperature

Figure 6 shows the effect of the heat source temperature on the coefficient of performance of the system. The heat source temperature was varied from 115 to 130 ^{o}C, with a 2.5 ^{o}C increment and at an entrainment ratio of 0.90. The results indicate that the COP of the cycle is slightly reduced with the increase of heat source temperature. With a higher thermal energy of the working fluid at the turbine inlet, the power output is increased. Thus, the net power requirement of the system is also decreased. However, the rate at which heat is supplied is greater than the decrease of the system power input. This may have caused the decrease of the COP of the system.

On the other hand, the effect of the heat source temperature on the exergy efficiency differs with the working fluids. The effects of the heat source temperature on the exergy efficiency is shown in Figure 7. For R123 and R141b, the exergy efficiency increases with higher heat source temperature. It is observed that the waste heat stream at the vapor generator exits at a lower temperature, which indicates better heat exchange and utilization of thermal energy for power production. Conversely, the exergy efficiency decreases for the system that uses R245fa. There is only a minimal effect on the exhaust heat source exergy. As the heat temperature is increased, the exergy input at the vapor generator is also increased that may result in the decrease of the exergy efficiency of the system.

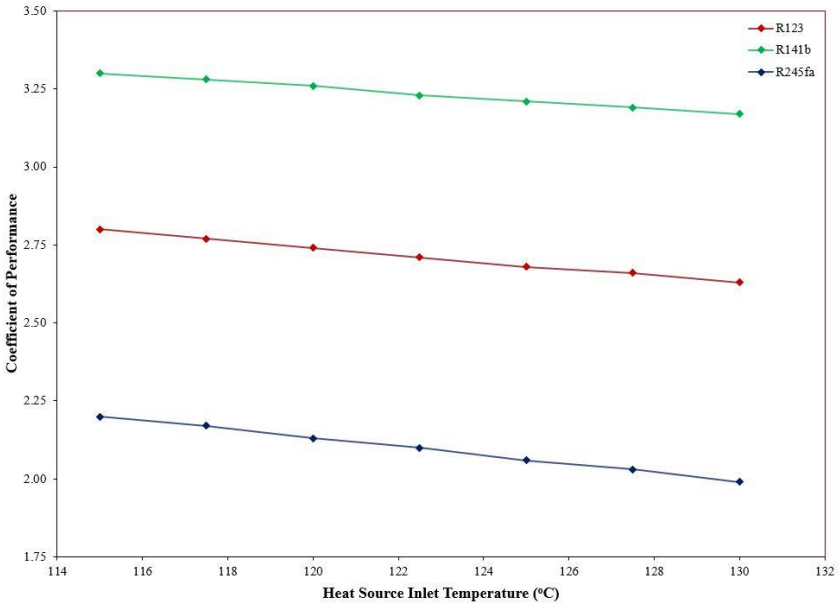

Figure 6. Effect of Heat Source Inlet Temperature on COP of the system

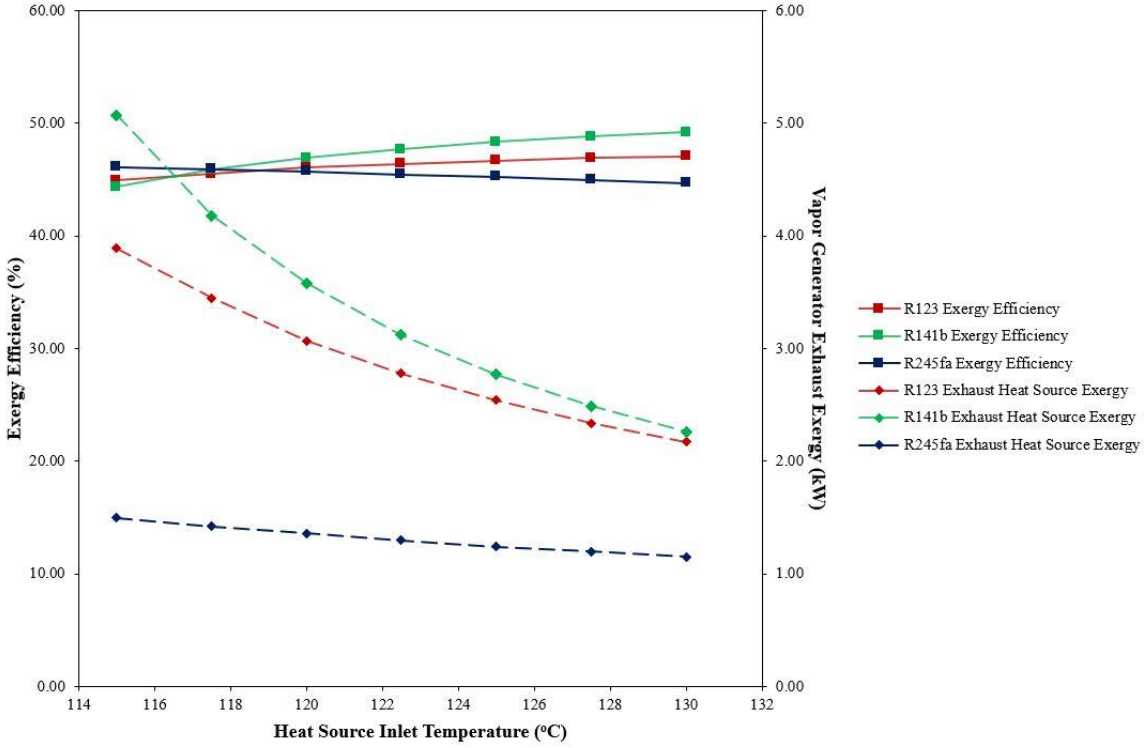

Figure 7. Effect of heat source temperature on the cycle η_{exg} and exhaust heat source exergy

5.3. Effects of Evaporator Temperature

The evaporator temperature was varied from -5 ^{o}C to 7.5 ^{o}C, while the values of other parameters are those specified in Table 1. Figure 8 shows the effects of the evaporating temperature on the power requirement and refrigeration exergy of the system. Both compressor and turbine power are reduced with higher evaporating temperatures. However, the rate of decrease in power required by the compressor is greater than the decrease in the power produced by the turbine. This may have resulted in lower power requirement of the system.

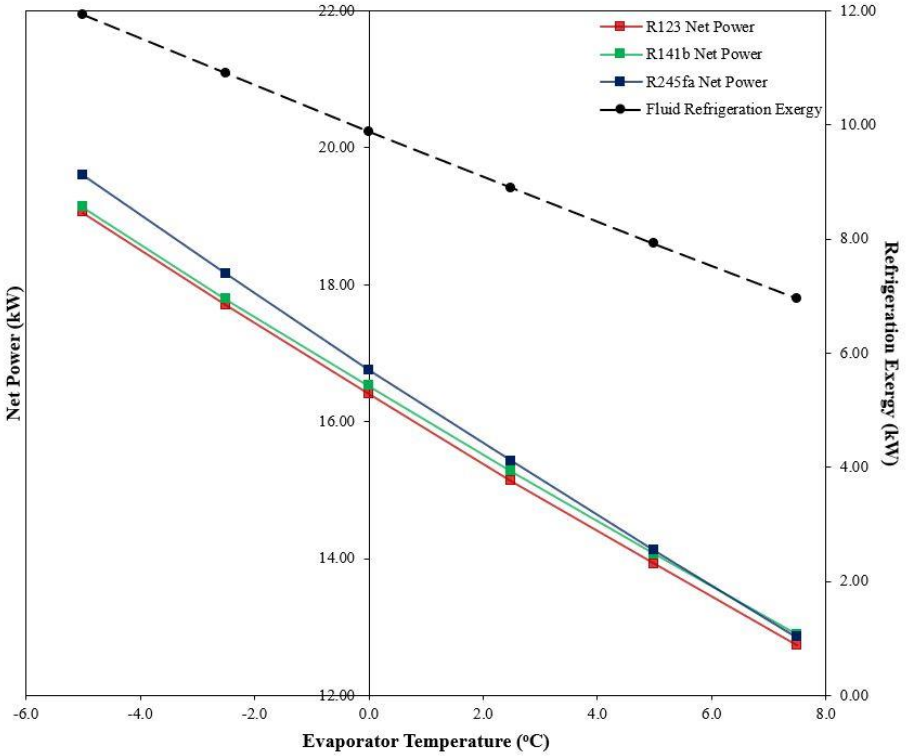

Figure 8. Effect of evaporator temperature on the power required by the system and on the refrigeration exergy

The effects of the evaporator temperature on the COP and exergy efficiency are shown in Figure 9. The COP of the system improves with the increase in evaporating temperature. Aside from lower power requirement, the heat duty at the vapor generator is also reduced. With lower values of both power and heat requirements of the system, the COP increased. However, the tradeoff of higher evaporating temperature is its lower refrigeration exergy which results in a lower exergy efficiency.

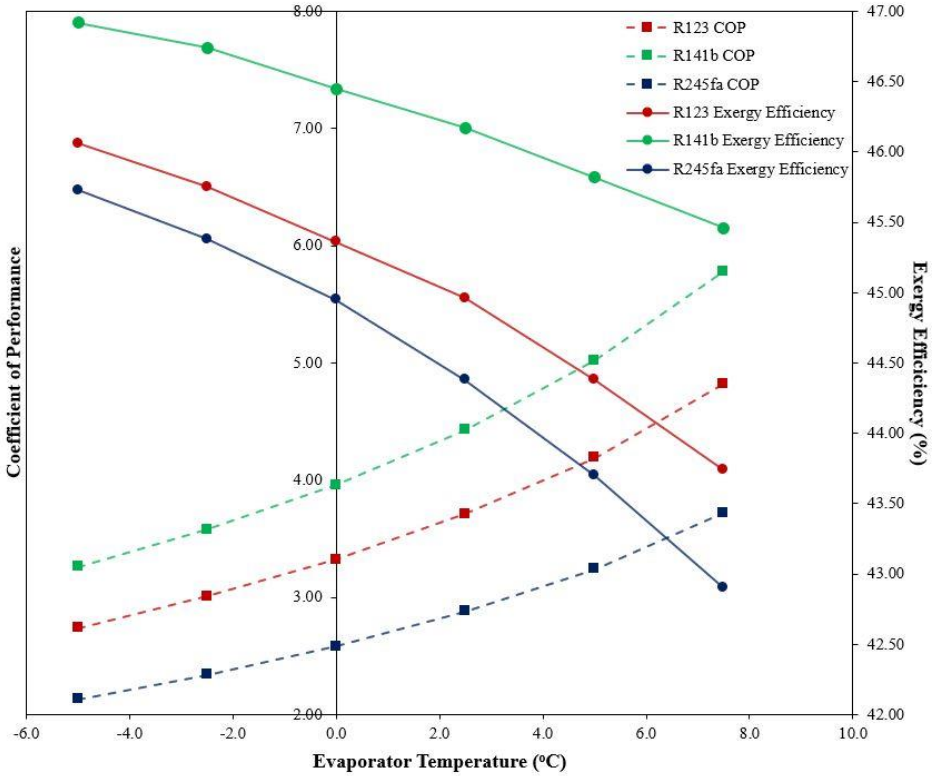

Figure 9. Effect of evaporator temperature on the COP and η_{exg} of the system

VII. CONCLUSION AND RECOMMENDATIONS

A novel combined cooling and power system is proposed by coupling an organic Rankine cycle and a compressor-driven ejector refrigeration cycle. A mathematical model was developed to investigate the performance of the proposed system using three working fluids namely R123, R141b, and R245fa. Among the working fluids, R141b had the highest coefficient of performance and exergy efficiency with values of 3.26 and 46.92%, respectively. Parametric analyses were also conducted to study the effects of the entrainment ratio, and the heat source and evaporator temperatures on the performance of the system. Among these parameters, the heat source temperature had the least effect on the COP and exergy efficiency. It is also concluded that the amounts of exergy destruction in the vapor generator, condenser, compressor, and turbine accounted for large percentage. Therefore, it is important to employ methods that will reduce the irreversibilities in these devices such as increasing the heat transfer area and heat transfer coefficient of the heat exchanger, and optimizing the compressor and turbine designs.

Initial theoretical analysis of the performance of the novel power-and-refrigeration system was conducted. Based on the simulations made, it is recommended to investigate the performance of the system on a wider range of parameters. It is observed that some fluids perform poorly on the set values of the parameters. It is also suggested to consider shock to simulate the actual conditions in an ejector. Moreover, it is recommended to conduct an

optimization analysis of different working parameters, and to explore the use of other fluids. Using more sophisticated thermo-fluid models and simulation packages, specially those that can handle two-phase flow well, and conducting experimental verifications are highly recommended for further research studies. As it is a preliminary study on the introduced novel system, experimental validation of the simulated flow behavior and performance of the system is in the plan for future studies.

NOMENCLATURE

c	specific heat at constant pressure (kJ kg^{-1} K^{-1})
COP	coefficient of performance (-)
E	exergy (kW)
h	specific enthalpy (kJ kg^{-1})
I	exergy destruction (kW)
$\dot{m}$	mass flow rate (kg s^{-1})
ORC	organic Rankine cycle
P	pressire (kPa)
$\dot{Q}$	thermal power (kW)
s	specific entropy (kJ kg^{-1} K^{-1})
T	temperature (K)
$\dot{W}$	mechanical power (kW)
x	quality of saturated mixture (-)

Greek symbols

η	efficiency (-)
ω	entrainment ratio

Subscripts

a	air
c	compressor
e	evaporator
exg	exergy
f	saturated liquid
g	saturated vapor
j	ejector
k	condenser
o	environment
p	pump
s	isentropic
sep	vapor-liquid separator
t	turbine
td	throttling device
vg	vapor generator
w	water

REFERENCES

[1] BCS Inc. (2008). Waste Heat Recovery: Technologies and Opportunities in U.S. Industry. U.S. Department of Energy (DOE).

[2] Republic of the Philippines Department of Energy (2015). 2015 Philippine Power Statistics. Retrieved November 30, 2016, from https://www.doe.gov.ph/sites/default/files/pdf/energy_statistics/power_statistics_2015_summary.pdf

[3] Lister, M. (2015). Philippines Energy Efficiency and Conservation Action Plan 2016-2020: Recommendations to the Philippine Department of Energy.

[4] Stricker, S., Strack, T., Monier, L. F., & Clayton, R. (2006). Market Report on Waste Heat and Requirements for Cooling and Refrigeration in Canadian Industry.

[5] Tchanche, B. F., Lambrinos, G., Frangoudakis, A., & Papadakis, G. (2011). Low-Grade Heat Conversion into Power Using Organic Rankine Cycles – A Review of Various Applications. Renewable and Sustainable Energy Reviews, 15(8), 3963–3979. https://doi.org/10.1016/j.rser.2011.07.024

[6] Description of the Industrial Waste Heat Utilisation with Consideration of an Optimised Power Production Based on an ORC. (n.d). Retrieved November 30, 2016, from www.bios-bioenergy.at/en/waste-heat-utilisation.html

[7] Collado, R., Peris, B., Navarro-esbrí, J., & Mol, F. (2015). Performance Evaluation of an Organic Rankine Cycle (ORC) for Power Applications from Low Grade Heat Sources, 75, 763–769. https://doi.org/10.1016/j.applthermaleng.2014.10.034

[8] Darawun, W., Songprakorp, R., & Monyakul, V. (2015). Testing of Low-Grade Heat Source Organic Rankine Cycle with Small Hot Vapor Reciprocating Engine. Energy Procedia (Vol. 79). Elsevier B.V. https://doi.org/10.1016/j.egypro.2015.11.497

[9] Peris, B. (2015). Experimental Study of an ORC (Organic Rankine Cycle) for Low Grade Waste Heat Recovery in a Ceramic Industry, 85, 534–542. https://doi.org/10.1016/j.energy.2015.03.065

[10] Banik, S., Ray, S., & De, S. (2016). Thermodynamic Modelling of a Recompression CO2 Power Cycle for Low Temperature Waste Heat Recovery. Applied Thermal Engineering, 107, 441–452. https://doi.org/10.1016/j.applthermaleng.2016.06.179

[11] Hsieh, J., Fu, B., Wang, T., Cheng, Y., Lee, Y., & Chang, J. (2017). Design and Preliminary Results of a 20-kW Transcritical Organic Rankine Cycle with a Screw Expander for Low-Grade Waste Heat Recovery, 110, 1120–1127.

[12] Li, L., Ge, Y. T., Luo, X., & Tassou, S. A. (2016). Thermodynamic Analysis and Comparison between CO2 Transcritical Power Cycles and R245fa Organic Rankine Cycles for Low Grade Heat to Power Energy Conversion, 106, 1290–1299. https://doi.org/10.1016/j.applthermaleng.2016.06.132

[13] Bao, H., Ma, Z., & Roskilly, A. P. (2017). Chemisorption Power Generation Driven by Low Grade Heat – Theoretical Analysis and Comparison with Pumpless ORC. APPLIED ENERGY, 186, 1–9. https://doi.org/10.1016/j.apenergy.2016.01.022

[14] Hoon, K., & Chun, K. (2014). Thermodynamic Performance Analysis of a Combined Power Cycle Using Low Grade Heat Source and LNG Cold Energy. Applied Thermal Engineering, 70(1), 50–60. https://doi.org/10.1016/j.applthermaleng.2014.04.064

[15] Kwon, K., Park, B. H., Kim, D. H., & Kim, D. (2015). Parametric Study of Reverse Electrodialysis Using Ammonium Bicarbonate Solution for Low-Grade Waste Heat Recovery. Energy Conversion and Management, 103, 104–110. https://doi.org/10.1016/j.enconman.2015.06.051

[16] Chen, Y., Han, W., & Jin, H. (2017). Proposal and Analysis of a Novel Heat-Driven Absorption-Compression Refrigeration System at Low Temperatures. Applied Energy, 185, 2106–2116. https://doi.org/10.1016/j.apenergy.2015.12.009

[17] Salmi, W., Vanttola, J., Elg, M., Kuosa, M., & Lahdelma, R. (2017). Using Waste Heat of Ship as Energy Source for an Absorption Refrigeration System. Applied Thermal Engineering, 115, 501–516. https://doi.org/10.1016/j.applthermaleng.2016.12.131

[18] Yang, S., Liang, J., Yang, S., & Qian, Y. (2016). A Novel Cascade Refrigeration Process Using Waste Heat and Its Application to Coal-to-SNG. Energy, 115, 486–497. https://doi.org/10.1016/j.energy.2016.09.039

[19] Alexis, G. K. (2007). Performance Parameters for the Design of a Combined Refrigeration and Electrical Power Cogeneration System. International Journal of Refrigeration, 30(6), 1097–1103. https://doi.org/10.1016/j.ijrefrig.2006.12.013

[20] Dai, Y., Wang, J., & Gao, L. (2009). Exergy Analysis, Parametric Analysis and Optimization for a Novel Combined Power and Ejector Refrigeration Cycle. Applied Thermal Engineering, 29(10), 1983–1990. https://doi.org/10.1016/j.applthermaleng.2008.09.016

[21] Zheng, B., & Weng, Y. W. (2010). A Combined Power and Ejector Refrigeration Cycle for Low Temperature Heat Sources. Solar Energy, 84(5), 784–791. https://doi.org/10.1016/j.solener.2010.02.001

[22] Yang, X., Zhao, L., Li, H., & Yu, Z. (2015). Theoretical Analysis of a Combined Power and Ejector Refrigeration Cycle using Zeotropic Mixture, Applied Energy, 160, 912–919. https://doi.org/10.1016/j.apenergy.2015.05.001

[23] Wang, J., Dai, Y., & Sun, Z. (2009). A Theoretical Study on a Novel Combined Power and Ejector Refrigeration Cycle. International Journal of Refrigeration, 32(6), 1186–1194. https://doi.org/10.1016/j.ijrefrig.2009.01.021

[24] Habibzadeh, A., Rashidi, M. M., & Galanis, N. (2013). Analysis of a Combined Power and Ejector-Refrigeration Cycle using Low Temperature Heat. Energy Conversion and Management, 65, 381–391. https://doi.org/10.1016/j.enconman.2012.08.020

[25] Garcia, J. C. S., Alcaraz, J. Y. T., Alvarez, J. R. A., Abuan, B. E., & Berana, M. S. (2014). Ejector Profile Modeling for Compressor-Driven Ejector Refrigeration System. Philippine Engineering Journal, XXXV (2), 38-56.

[26] Borgnakke, C., & Sonntag, R.E. (2013). *Fundamentals of Thermodynamics* (8th ed.). John Wiley & Sons, Inc.

[27] Bell, I. H., Wronski, J., Quoilin, S., & Lemort, V. (2014). Pure and Pseudo-Pure Fluid Thermophysical Property Evaluation and the Open-Source Thermophysical Property Library CoolProp. Industrial & Engineering Chemistry Research, 53(6), 2498–2508. https://doi.org/10.1021/ie4033999

[28] Joseph, D.D., & Yang, B.H. (2010). Friction Factor Correlations for Laminar, Transition, and Turbulent Flow in Smooth Pipes. Physica D: Nonlinear Phenomena, 239(14), 1318-1328. https://doi.org/10.1016/j.physd.2009.09.026.

[29] Berana, M.S., & Bermido, E.T. (2013). Design and Analysis of Ejector Powerplant System. Proceedings of the ASME 2013 International Mechanical Engineering Congress and Exposition (IMECE 2013), San Diego, California, USA. https://doi.org/10.1115/IMECE2013-65130.

[30] Espeña, G.D., & Berana, M.S. (2013). Ejector Modeling for Heat-Driven Ejector Refrigeration System. Proceedings of the 8th International Conference on Multiphase Flow (ICMF 2013), Jeju, South Korea.

[31] Redo, M.A.B., Berana, M.S., & Espeña, G.D. (2013). Mathematical Model of Irreversible Nozzle Condition for Heat-Driven Ejector Refrigeration System. Proceedings of the 8th International Conference on Multiphase Flow (ICMF 2013), Jeju, South Korea.

[32] Berana, M.S. (2005). Characteristics of Supersonic Two-Phase Flow of Carbon Dioxide through a Converging-Diverging Nozzle of an Ejector in a Refrigeration Cycle [Unpublished master's thesis]. Toyohashi University of Technology, Toyohashi, Aichi, Japan.

[33] Berana. M.S. (2009). Characteristics and Shock Waves of Supersonic Two-Phase Flow of CO2 through Converging-Diverging Nozzles [Unpublished doctoral dissertation]. Toyohashi University of Technology, Toyohashi, Aichi, Japan.

[34] Centrum voor Wiskunde en Informatica. (1995). Python tutorial. Technical Report CS-R9526.